

## Growth and Characterization of All-inorganic Perovskite CsPbBr<sub>3</sub> Crystal by a Traveling Zone Melting Method

XU Jia-Yue<sup>1</sup>, LIANG Xiao-Xiao<sup>1</sup>, JIN Min<sup>2</sup>, ZENG Hai-Bo<sup>1,3</sup>, KIMURA Hideo<sup>4</sup>,  
HU Hao-Yang<sup>2</sup>, SHAO He-Zhu<sup>2</sup>, SHEN Hui<sup>1</sup>, TIAN Tian<sup>1</sup>, LI Hai-Xia<sup>1</sup>

(1. Institute of Crystal Growth, School of Materials Science and Engineering, Shanghai Institute of Technology, Shanghai 201418, China; 2. College of Materials, Shanghai Dianji University, Shanghai 201306, China; 3. Institute of Optoelectronics and Nanomaterials, College of Materials Science and Engineering, Nanjing University of Science and Technology, Nanjing 210094, China; 4. National Institute for Materials Science, 1-2-1 Sengen, Tsukuba, Ibaraki 305-0047, Japan)

**Abstract:** A self-designed traveling zone melting method was employed to fabricate perovskite CsPbBr<sub>3</sub> crystals, which is helpful for impurities removing and moisture excluding. A large-size CsPbBr<sub>3</sub> crystal with a dimension of  $\phi 25$  mm $\times$  60 mm is successfully obtained. The as-grown crystal shows orange color and displays an excellent transmittance of 78.6% in the range of 600 nm – 2000 nm wavelength. It is revealed by DSC analysis that there is phase transition at 88.1 $^{\circ}$ C and 131.25 $^{\circ}$ C, respectively. The band gap  $E_g$  of the crystal is calculated to be 2.25 eV. The above results prove that the traveling zone melting method is indeed a potential approach for large size and high quality CsPbBr<sub>3</sub> crystal preparation.

**Key words:** traveling zone melting method; CsPbBr<sub>3</sub> crystal; transmittance; band gap

During the past several years, a series of all-inorganic version of the lead bromide perovskite (CsPbX<sub>3</sub>, X= Cl, Br, I) has attracted great attention due to its outstanding performance and broad potential applications in optoelectronic fields<sup>[1-6]</sup>. Among them, cesium lead bromine (CsPbBr<sub>3</sub>) is a representative material. For example, the mobility lifetime product  $\mu\tau$  of CsPbBr<sub>3</sub> crystal for electrons could up to  $1.7\times 10^{-3}$  cm<sup>2</sup>/V that is comparable to the CdZnTe crystal, and the  $\mu\tau$  value for holes is  $1.3\times 10^{-3}$  cm<sup>2</sup>/V which is about ten times higher than that of CdZnTe, such excellent properties make CsPbBr<sub>3</sub> crystal a promising candidate material for X- and  $\gamma$ -ray radiation detection at room temperature<sup>[2]</sup>. Besides, the measured high resistivity (343 G $\Omega$ ·cm) implies it is favorable for photon detection<sup>[7]</sup>. In addition, CsPbBr<sub>3</sub> crystal is also considered as a fast decay scintillator as its decay time is only 10 ps–20 ps<sup>[8-9]</sup>. Based on the bright application prospect, the preparation of large and high quality CsPbBr<sub>3</sub> crystal has become much significant. However, it is regrettable that the obtained CsPbBr<sub>3</sub> crystals are always in small size although many growth techniques have been employed in past years. For example, Stoumpos, *et al*<sup>[2]</sup> fabricated CsPbBr<sub>3</sub> crystal *via* a vertical Bridgman method, but the as-grown crystal is only about  $\phi 7$  mm $\times$

12 mm in dimensions. Zhang, *et al*<sup>[10]</sup> conducted crystal growth by a creative electronic dynamic gradient (EDG) method and the crystal is about  $\phi 8$  mm $\times$ 58 mm. Rakita *et al*<sup>[11]</sup> produced CsPbBr<sub>3</sub> crystals through a solution-grown method under a low temperature condition (90 $^{\circ}$ C–110 $^{\circ}$ C), however, the largest crystal is millimeter-sized. Therefore, it is obvious that some novel techniques are still expected to grow CsPbBr<sub>3</sub> crystal. In this work, a self-designed traveling zone melting method is introduced and a large-size CsPbBr<sub>3</sub> crystal about  $\phi 25$  mm $\times$  60 mm in dimensions is successfully produced, besides, the crystal quality and its properties are also investigated.

## 1 Experiment

### 1.1 Synthesis of CsPbBr<sub>3</sub> polycrystalline

CsPbBr<sub>3</sub> polycrystalline was synthesized from 99.99% purity of CsBr and PbBr<sub>2</sub> powders with mole ratio of 1 : 1 (the total weight was about 132 g). Considering CsBr and PbBr<sub>2</sub> were both water sensitive, the weighting and loading process was conducted under N<sub>2</sub> atmosphere in a glove box. The raw materials were loaded into a  $\phi 25$  mm quartz tube which was carefully cleaned by

**Received date:** 2018-05-21; **Modified date:** 2018-07-16

**Foundation item:** National Natural Science Foundation of China (51472263, 51572175, 61605116); Ningbo Natural Science Foundation (2017A610009); Public Projects of Zhejiang Province (2017C31006); Shanghai Natural Science Foundation (15ZR1440600)

**Biography:** XU Jia-Yue (1966–), professor. E-mail: xujiayue@sit.edu.cn

**Corresponding author:** JIN Min, professor. E-mail: jmaish@aliyun.com

aqua regia and  $\sim 18 \text{ M}\Omega\text{-cm}$  DI water. The quartz tube was sealed by oxyhydrogen flame with  $<10^{-3} \text{ Pa}$  vacuum, then, it was placed into a rocking furnace. The furnace temperature was controlled at  $620^\circ\text{C}$  that was about  $50^\circ\text{C}$  higher than the melting point of  $\text{CsPbBr}_3$ . After the raw materials were melted and soaked for half an hour, the rocking system was started to work at a rate of 30 r/min for 20 min to enhance  $\text{CsPbBr}_3$  synthesis homogeneous. Finally, the furnace was naturally cooled to room temperature. Table 1 lists the parameters for  $\text{CsPbBr}_3$  polycrystalline synthesis. Fig. 1 is the obtained  $\text{CsPbBr}_3$  polycrystalline that kept in quartz tube, the polycrystalline exhibited brown color and was easily separated from quartz wall. Importantly, no cracking phenomenon was found in the quartz tube, which implied the following crystal growth *via* such quartz tube would be safe.

## 1.2 Crystal growth

Before crystal growth, the volatility behavior of  $\text{CsPbBr}_3$  was suggested to be clarified that would do benefit to guide the choice of furnace temperature. Fig. 2

**Table 1** Conditions for  $\text{CsPbBr}_3$  polycrystalline synthesis and crystal growth

Materials	Method	Conditions
$\text{CsPbBr}_3$ polycrystalline Synthesis	Synthesis method	Rocking technique
	Raw material	99.99% CsBr and $\text{PbBr}_2$ , 132 g
	Crucible	Quartz tube
	Vacuum	$<10^{-3} \text{ Pa}$
	Synthesis temperature	$620^\circ\text{C}$
	Rocking rate	30 r/min
	Rocking time	20 min
	$\text{CsPbBr}_3$ crystal growth	Growth method
Crucible		Quartz tube
Vacuum		$<10^{-3} \text{ Pa}$
Furnace temperature		$585^\circ\text{C}$
Temperature gradient		$30^\circ\text{C}/\text{cm}-40^\circ\text{C}/\text{cm}$
Growth rate		1.0 mm/h
Cooling rate		$50^\circ\text{C}/\text{h}$



Fig. 1 Synthesized  $\text{CsPbBr}_3$  polycrystalline

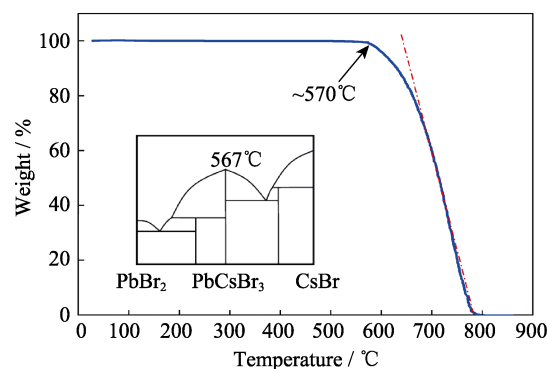


Fig. 2 TG curve of  $\text{CsPbBr}_3$  material

shows the relationship between weight percentage and temperature examined by thermogravimetry equipment (TG-DTA 8121, Japan) with  $5^\circ\text{C}/\text{min}$  increasing rate. It was observed no weight losing took place from room temperature to  $570^\circ\text{C}$ . The result means  $\text{CsPbBr}_3$  is stable under melting point (see inserted  $\text{PbBr}_2$ - $\text{CsBr}$  phase diagram in Fig. 2). However, as temperature was continuously increased, the weight percentage was decreased sharply. Based on the TG curve, the average volatilization speed above melting point was calculated to be  $\sim 2.5\%$  per minute. Finally,  $\text{CsPbBr}_3$  was totally exhausted as temperature reached  $800^\circ\text{C}$ . Such behavior illustrated that  $\text{CsPbBr}_3$  was easily volatilized above melting point. Therefore, the furnace temperature for  $\text{CsPbBr}_3$  crystal growth should be designed as low as possible.

Fig. 3(a) shows the schematic diagram of the self-designed traveling zone melting furnace. It was heated by winding Fe-Cr-Al resistance wires which were located in middle position of furnace. The furnace temperature was detected by a couple of Pt/Pt-10%Rh thermocouples and monitored *via* DWT-702 with a proportional integral differential (PID) controller. In this experiment, the furnace temperature was set as  $585^\circ\text{C}$ . Fig. 3(b) is the temperature profile along vertical direction, and the melting zone was only 20 mm–25 mm in height.  $\text{CsPbBr}_3$  polycrystalline with vacuumed quartz tube was placed on a steel support. A Pt/Pt-10%Rh thermocouples were installed near the bottom of quartz tube for indicating the temperature of  $\text{CsPbBr}_3$  polycrystalline/melt. After the  $\text{CsPbBr}_3$  polycrystalline was melted and soaked for 8 h, the motor system was started to work and the furnace was traveled upward with 1.0 mm/h speed. Then,  $\text{CsPbBr}_3$  crystal growth was started and the temperature gradient in the solid-liquid interface was about  $30-40^\circ\text{C}/\text{cm}$ . Finally, after all of the solution was crystallized, the furnace was cooled down to room temperature at a rate of  $50^\circ\text{C}/\text{h}$ . The parameters for  $\text{CsPbBr}_3$  crystal growth were listed in Table 1.

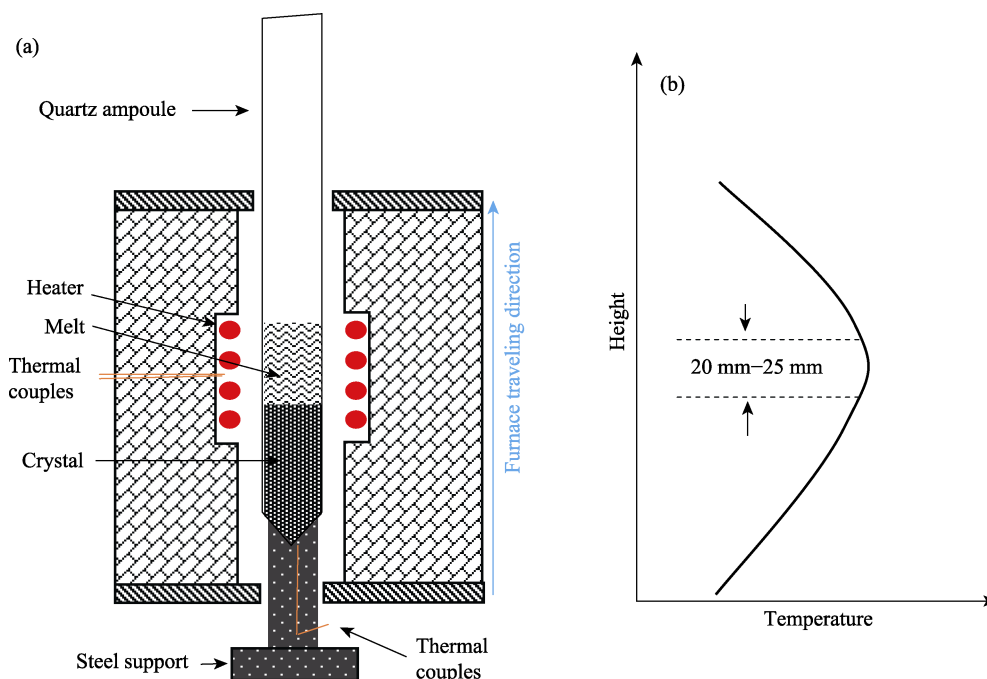


Fig. 3 Schematic diagram of CsPbBr<sub>3</sub> crystal growth (a) and temperature profile along vertical direction in the furnace (b)

### 1.3 Characterization

Phase structure of the samples were analyzed by X-ray diffraction (Bruker D8, Germany) using CuK $\alpha$  radiation ( $\lambda=0.15406$  nm) at room temperature. Crystal cutting was carried out by a diamond wire cutting machine (STX-1202A, China) using absolute alcohol as lubricant to prevent CsPbBr<sub>3</sub> from moisture absorption. CsPbBr<sub>3</sub> wafers are ground by 200  $\mu\text{m}$  SiC powder and polished by 20  $\mu\text{m}$  Al<sub>2</sub>O<sub>3</sub> powder. Phase transition temperature is tested by Differential Scanning Calorimetry (Flash DSC 2+, China). Crystal transmittance and diffuse reflection are analyzed by ultraviolet visible near infrared spectrophotometer (LAMBDA, China).

## 2 Results and discussion

Benefit from zone melting temperature profile of the furnace, there are two outstanding advantages for CsPbBr<sub>3</sub> crystal growth in this experiment: (i) The existing impurities in raw material could be removed from bottom to top gradually, as shown in Fig. 4(a). Some black impurities are noticed on tail part of the ingot; (ii) Most of the water could be excluded due to the special furnace temperature distribution, and the excluded water is re-condensed on the cold part of quartz tube, as shown in Fig. 4(b). Large size CsPbBr<sub>3</sub> crystal with a dimension of about  $\phi 25$  mm  $\times$  60 mm was shown in Fig. 5(a) and (b) are some samples cut from the ingot. The as-grown crystal and the cutting samples display orange color and look uniformity.

Fig. 6(a) is the XRD powder diffraction diagram of

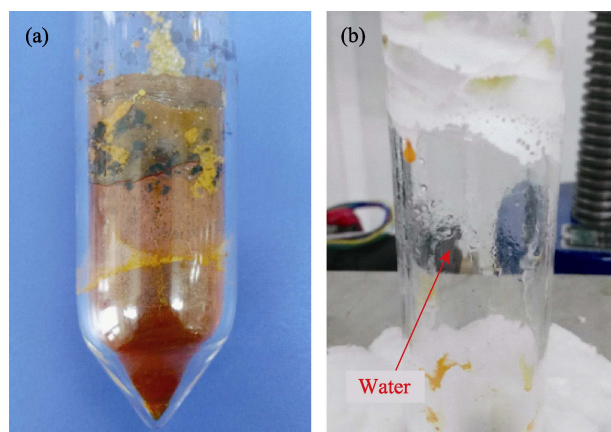


Fig. 4 As-grown CsPbBr<sub>3</sub> crystal in quartz tube (a) and attached water on the inside wall of quartz (b)

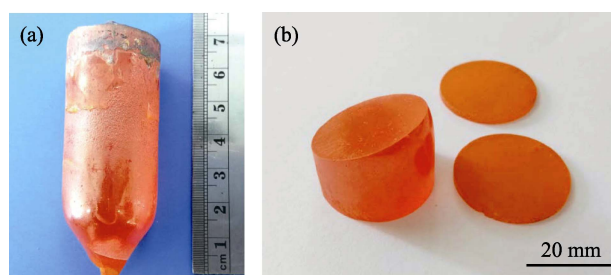


Fig. 5 As-grown CsPbBr<sub>3</sub> crystal (a) and some cutting samples (b)

the as-grown crystal. It is found that all the diffraction patterns can be indexed as the room temperature CsPbBr<sub>3</sub> phase (PDF#18-0364), indicating an *Pnma* space group, and the crystal lattices are calculated to be  $a=0.8205$  nm,  $b=0.8250$  nm and  $c=1.1754$  nm. To evaluate the crystallinity

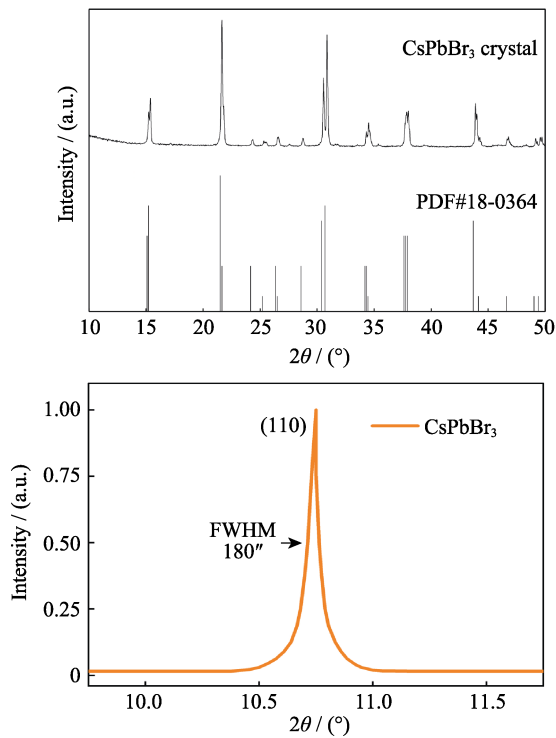


Fig. 6 XRD patterns of CsPbBr<sub>3</sub> crystal powders (a) and the rocking curve of CsPbBr<sub>3</sub> crystal

of as-grown crystal, the double rocking curve was measured by DX-9BG X-ray orientation. Fig. 6(b) shows the rocking curve with the central peak at 10.75°, which corresponds to the (110) diffraction peak. The full width at half maximum of the peak (FWHM) is about 180 arc sec.

Fig. 7 exhibits the DSC thermal analysis results with temperature from 30°C to 350°C. As the temperature is increased, there are two endothermic peaks at 89.1°C and 132.9°C, respectively, which correspond to the phase transitions to tetragonal (P4/mbm) and cubic (Pm3m). On the contrary, as the temperature is decreased, two exothermic peaks appeared at 87.1°C and 129.6°C, respectively. This result means the phase transitions of CsPbBr<sub>3</sub> crystal are reversible. Considering the slight different transform temperature, we define here that the average

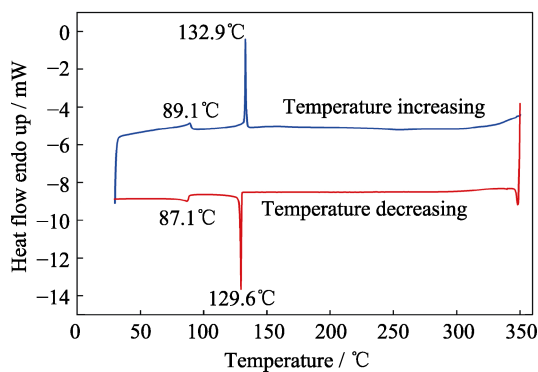


Fig. 7 DSC thermal analysis of CsPbBr<sub>3</sub> crystal

phase transition point  $T_{OT}$  for Orthorhombic (Pnma) to Tetragonal (P4/mbm) is 88.1°C, and the value  $T_{TC}$  for Tetragonal (P4/mbm) to Cubic (Pm3m) is 131.25°C.

Fig. 8 is the transmittance spectrum of CsPbBr<sub>3</sub> crystal in the range of 200 nm-2000 nm wavelength. It is noticed that the crystal is absolutely opaque under 543 nm which corresponds to its absorption edge. Then, the transmittance is rapidly raised as wavelength increasing. For example, when wavelength reaches 570 nm, the transmittance value arrives at 63.2%. Subsequently, as wavelength continuously increases, the transmittance increasing tendency becomes moderately, and the highest value is about 78.6% in the range of 600 nm-2000 nm wavelength. In fact, the insert figure showed good transmittance in visible light, which means the as-grown crystal has better quality than the samples in literatures<sup>[2,7]</sup>.

Fig. 9(a) is the diffuse reflection spectroscopy of CsPbBr<sub>3</sub> powder in the range of 200 nm-1800 nm wavelength. According to Kubelka-Munk equation<sup>[12]</sup>:

$$F[R] = (1-R)^2 / 2R \quad (1)$$

Where  $R$  is diffuse reflection ratio. The band gap  $E_g$  of CsPbBr<sub>3</sub> can be induced from the relationship of  $[F(R)hv]^{1/2}$  with  $hv$  as CsPbBr<sub>3</sub> is considered to be a direct band gap semiconductor<sup>[2]</sup>. As a result, the  $E_g$  of CsPbBr<sub>3</sub> is calculated to be 2.25 eV (in Fig. 9(b)).

In Table 2, we summarized the growth results of the present work compared with other CsPbBr<sub>3</sub> crystals grown by various methods. It is concluded that the crystal size in this work is the largest that implies such traveling zone melting method is indeed a simple and effective approach for CsPbBr<sub>3</sub> crystal preparation. Besides, some of their properties, including crystal structure, phase transition temperature and band gap are found basically the same, however, the present CsPbBr<sub>3</sub> crystal displays relative higher transmission performance, which proves this crystal growth technique is a better choice for high quality CsPbBr<sub>3</sub> crystal fabrication in the future.

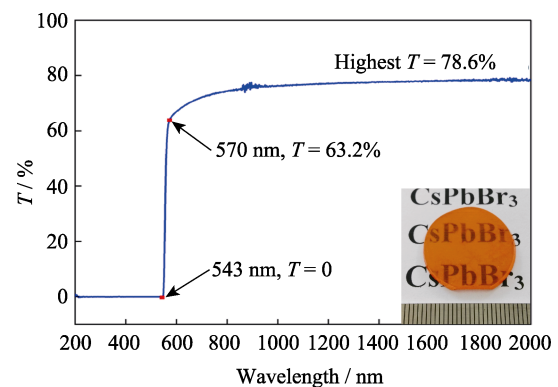
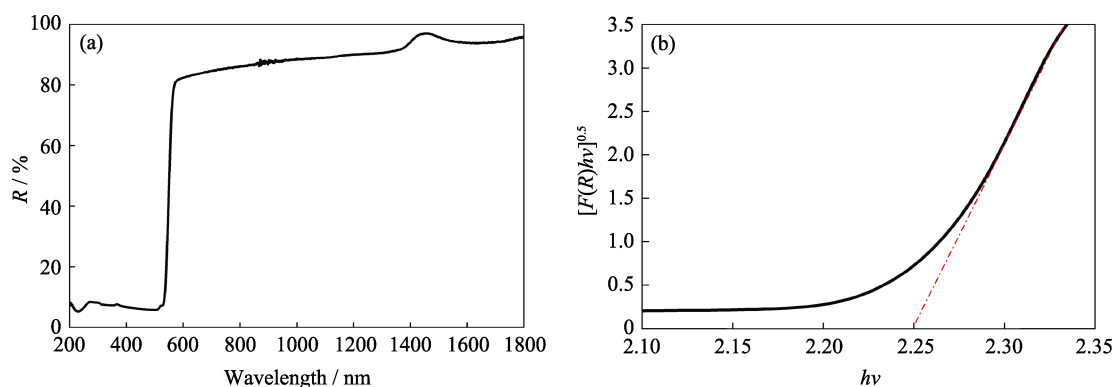


Fig. 8 Transmittance spectrum of CsPbBr<sub>3</sub> crystal

Fig. 9 Diffuse reflection spectroscopy of CsPbBr<sub>3</sub> (a) and transformed Kubelka–Munk spectrum of CsPbBr<sub>3</sub> (b)**Table 2 Growth results and properties of CsPbBr<sub>3</sub> crystal**

Growth method	Crystal size/mm <sup>3</sup>	Color	Band gap, $E_g$ /eV	Highest transmittance/%	Phase transition temperature/°C		Ref.
Traveling zone melting	$\phi 25 \times 60$	Orange	2.250	78.6	Orthorhombic → Tetragonal 88.1	Tetragonal → Cubic 131.25	This work
Vertical Bridgman	$\phi 7 \times 12$	Orange	2.250	—	88	130	[2]
Solution grown	$7 \times 2 \times 4$	Orange	2.254	—	—	—	[11]
Electronic dynamic gradient	$\phi 8 \times 58$	Orange	2.252	75	87	127	[10]

### 3 Conclusions

In this work, a self-designed traveling zone melting method was adopted to grow CsPbBr<sub>3</sub> crystal and the CsPbBr<sub>3</sub> polycrystalline was synthesized in advance for impurities removing and moisture excluding due to the special temperature distribution. By optimizing growth conditions, a large size CsPbBr<sub>3</sub> crystal up to 25 mm in diameter and 60 mm in length was obtained. The as-grown crystal displays orange color and excellent transmittance. The crystal structure, phase transition point and band gap are investigated in accordance well with the literatures previously reported. The growth results imply the traveling zone melting method is indeed a better choice for large and high quality CsPbBr<sub>3</sub> crystal growth.

### References:

- [1] YETAPU G R, TALUKDAR D, SARKAR S, et al. THz conductivity within colloidal CsPbBr<sub>3</sub> perovskite nanocrystals: remarkably high carrier mobilities and large diffusion lengths. *Nano Letters*, 2016, **16**(8): 4838–4848.
- [2] STOUMPOS C C, MALLIAKAS C D, PETERS J A, et al. Crystal growth of the perovskite semiconductor CsPbBr<sub>3</sub>: a new material for high-energy radiation detection. *Crystal Growth & Design*, 2013, **13**(7): 2722–2727.
- [3] AKKERMAN Q A, D'INNOCENZOV, ACCORNERO S, et al. Tuning the optical properties of cesium lead halide perovskite nanocrystals by anion exchange reactions. *Journal of the American Chemical Society*, 2015, **137**(32): 10276–10281.
- [4] KANG J, WANG L W. High defect tolerance in lead halide perovskite CsPbBr<sub>3</sub>. *Journal of Physical Chemistry Letters*, 2017, **8**(2): 489–493.
- [5] HUANG H, BODNARCHUK M I, KERSHAW S V, et al. Lead halide perovskite nanocrystals in the research spotlight: stability and defect tolerance. *ACS Energy Letters*, 2017, **2**(9): 2071–2083.
- [6] LIU Z, PETERS J A, STOUMPOS C C, et al. Heavy Metal Ternary Halides for Room-temperature X-ray and Gamma-ray Detection. *SPIE Conference on Hard X-Ray, Gamma-ray, and Neutron Detector Physics XV*, 2013, **8852**: 88520A.
- [7] DIRIN D N, CHERNIUKH I, YAKUNIN S, et al. Solution-grown CsPbBr<sub>3</sub> perovskite single crystals for photon detection. *Chemistry of Materials*, 2016, **28**(23): 8470–8474.
- [8] HAMPLOVA V, NIKL M, POLAK K, et al. Lead bromide and ternary alkali lead bromide single crystals—growth and emission properties. *Chemical Physics Letters*, 1996, **258**(3): 518–522.
- [9] NIKL M, MIHOKOVA E, NITSCH K, et al. Photoluminescence and decay kinetics of CsPbCl<sub>3</sub> single crystals. *Chemical Physics Letters*, 1994, **220**(1/2): 14–18.
- [10] ZHANG M, ZHENG Z, FU Q, et al. Synthesis and single crystal growth of perovskite semiconductor CsPbBr<sub>3</sub>. *Journal of Crystal Growth*, 2017, **484**: 37–42.
- [11] RAKITA Y, KEDEM N, GUPTA S, et al. Low-temperature solution-grown CsPbBr<sub>3</sub> single crystals and their characterization. *Crystal Growth & Design*, 2016, **16**(10): 5717–5725.
- [12] MORALES A E, MORA E S, PAL U. Use of diffuse reflectance spectroscopy for optical characterization of unsupported nanostructures. *Revista Mexicana De Fisica*, 2007, **53**(78): 18–22.

# 移动区熔法生长全无机钙钛矿型 $\text{CsPbBr}_3$ 晶体及其性能研究

徐家跃<sup>1</sup>, 梁肖肖<sup>1</sup>, 金敏<sup>2</sup>, 曾海波<sup>1,3</sup>, KIMURA Hideo<sup>4</sup>,  
胡皓阳<sup>2</sup>, 邵和助<sup>2</sup>, 申慧<sup>1</sup>, 田甜<sup>1</sup>, 李海霞<sup>1</sup>

(1. 上海应用技术大学 材料科学与工程学院, 晶体生长研究所, 上海 201418; 2. 上海电机学院 材料学院, 上海 201306; 3. 南京理工大学 材料科学与工程学院, 纳米光电材料研究所, 南京 210094; 4. National Institute for Materials Science, 1-2-1 Sengen, Tsukuba, Ibaraki 305-0047, Japan)

**摘要:** 利用自制移动区熔炉生长了  $\text{CsPbBr}_3$  晶体, 事先采用相同工艺合成了高纯多晶原料以去除杂质和水分。通过工艺优化获得了大尺寸  $\text{CsPbBr}_3$  晶体, 达到  $\phi 25 \text{ mm} \times 60 \text{ mm}$ 。该晶体呈橘红色, 在 600~2000 nm 波长范围内具有透过率达 78.6% 的优异透光性能。热分析表明, 所得  $\text{CsPbBr}_3$  晶体在 88.1°C 和 131.25°C 时存在正交-四方和四方-立方相变。计算得到  $\text{CsPbBr}_3$  晶体的带宽  $E_g = 2.25 \text{ eV}$ 。上述结果表明移动区熔法是一种具有应用潜力的制备高质量大尺寸  $\text{CsPbBr}_3$  晶体的生长方法。

**关键词:** 移动区熔法;  $\text{CsPbBr}_3$  晶体; 透过率; 带隙

中图分类号: TQ174 文献标识码: A